

Continuous Flow Bioconjugations of NIR-AZA Fluorophores via Strained Alkyne Cycloadditions with Intra-chip Fluorogenic Monitoring

Sheila Fitzgerald and Donal F O'Shea*

Department of Chemistry, RCSI, 123 St Stephen's Green, Dublin 2, Ireland

***Email donalfoshea@rcsi.ie**

SF: orcid.org/0000-0003-3251-4754. DFOS: orcid.org/0000-0003-0594-4193.

Abstract

The importance of bioconjugation reactions continues to grow as the need for cell specific targeting and dual therapeutic plus diagnostic medical applications increase. This necessitates new bioconjugation chemistries, synthetic and analytical methods. With this goal, continuous flow bioconjugations were readily achieved with short residence times for strained alkyne substituted carbohydrate and peptide biomolecules in reaction with azide and tetrazine substituted fluorophores. The catalyst and reagent-free inverse electron demand tetrazine cycloadditions proved more favourable than the azide 1,3-dipolar cycloadditions. The use of a fluorogenic tetrazine fluorophore in a glass channelled reactor chip allowed for intra-chip reaction monitoring by recording fluorescence intensities at various positions throughout the chip. As the Diels-Alder reactions proceeded through the chip, the fluorescence intensity increased accordingly in real-time. This novel approach to continuous flow bioconjugation reaction with monitoring may offer advantages over post-chip analysis.

Introduction

Near infrared (NIR) fluorescence imaging is a dynamic research field fuelled by continued advancements in molecular probes and labelling.¹ The value of NIR-fluorescence imaging lies in its ability to visualise complex and dynamic biological systems in real-time from the nanometre (nm) to millimetre (mm) scale.^{2,3} At the higher nm resolution, research insights into subcellular function can be obtained, whereas at mm resolutions differentiation of tissues in living organisms is achievable. It is at the lower mm scale that there is potential for medical translational value in guiding surgical resections.⁴ The use of NIR-fluorescence in oncology is growing at a rapid pace as it has the ability to produce fluorescence tissue images in real-time during cancer operations. These images can improve surgical outcomes by defining tumour boundaries, thereby assisting in the removal of all the cancerous growth.⁵ The first clinical attempts to achieve this suffered from a lack of fluorophore / cancer specificity which has led researchers to explore fluorophores covalently conjugated to targeting motifs such as peptides, antibodies and synthetic polymers. Several of these agents are showing varying degrees of success in clinical trials.⁶ With this in mind, we believe it is worthwhile to begin exploring how the key covalent couplings between fluorophore and targeting motif could be performed most efficiently.⁷ As it would be expected that these contrast agents are administered only once and in small doses, their production would be favourably suited to flow synthesis. In addition, optimized flow methods could allow reaction times and conditions to be as biomolecule friendly as possible. The BF₂ chelated tetraarylazadipyrromethene (NIR-AZA) class of fluorophores **1** offer a robust and adaptable framework from which optimal physical and chemical attributes can be obtained through synthetic modifications (Fig. 1).^{8,9}

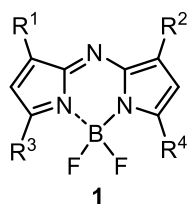


Fig. 1. Customizable framework of BF₂-azadipyrromethene (NIR-AZA) fluorophores **1**.

Reactive handles can be introduced to allow their covalent attachment to biomolecules or therapeutics to provide targeted imaging of specific biological regions of interest. To date, NIR-AZA derivatives containing activated ester, maleimide, azide, and strained alkynes have been used for this purpose.¹⁰⁻¹³ Peptide, antibody and carbohydrates biomolecules and therapeutics have been labelled with NIR-AZA fluorophores and used for *in vitro* cellular and *in vivo* small animal uses.^{8,14,15} The goal for this piece of work was to exploit the mild conditions of azide and tetrazine cycloadditions to develop bioconjugations, in continuous flow, using the NIR-AZA derivatives **2** and **3** as representative examples (Fig. 2).

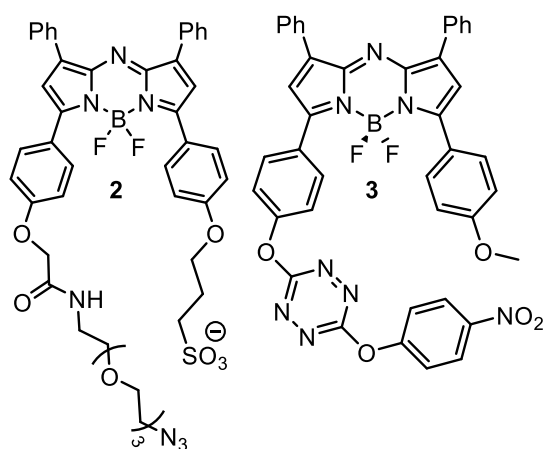
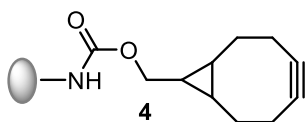


Fig. 2. NIR-AZA derivatives with azide **2** and tetrazine **3** cycloaddition reactive functional groups.

The bicyclo[6.1.0]non-4-yne (BCN) was chosen as the corresponding reacting strained alkyne unit with biomolecules functionalized as graphically shown in Fig. 3A. It was anticipated that the relatively low BCN lipophilicity would be advantageous for biomolecule functionalization and substrates could be tested with both **2** and **3** due to its good reaction kinetics for both azide 1,3-dipolar cycloadditions (ADC) and tetrazine inverse electron demand Diels Alder (iEDDA) reactions.¹⁸ The fluorogenic nature of the NIR-AZA tetrazine **3** provided an additional benefit for this study.¹⁶ A key feature of fluorogenic substrates is their low fluorescence quantum yields, only becoming strongly fluorescent when they react or bind with a specific substrate. Fluorogenic probes, which modulate their emission from off to on in response to bioorthogonal reactions, are highly valued for bio-assays and cellular fluorescence imaging.¹⁷ In the case of **3**, the tetrazine moiety causes excited state quenching but upon cycloaddition reaction, the quenching effect is

lost as the product is strongly fluorescent. It was anticipated that this additional feature would be of value as a means of following reaction progress based on intra-chip fluorescence intensities (Fig. 3B).

A BCN---biomolecule



B fluorogenic reaction monitoring

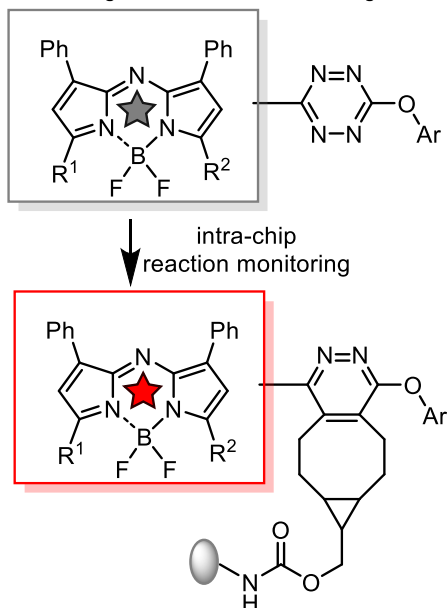


Fig. 3. Bioconjugation reacting stained alkyne and fluorogenic reaction monitoring. **A)** BCN substituted biomolecules; **B)** Fluorogenic bioconjugation of tetrazine substituted NIR-AZA.

Flow chemistry is an operational mode of synthetic chemistry that continues to gain in popularity.¹⁹ In flow, micro-reactor channels that are typically a fraction of a mm in diameter take the place of traditional batch reaction vessels. The small dimensions of the reactor channels allow for more efficient heat transfer, resulting in greater precision of reaction conditions and times. Furthermore, the micro-reactor technology has attractive safety, environmental and economic benefits. Reaction scale-up can be readily achieved by continually running the process for longer periods, termed scaling-out.²⁰ Flow reaction products are most often analysed after the reaction mixture exits the reactor (e.g. by HPLC, UV-Vis, MS) but if narrow glass channels are

used in the flow reactor this offers the possibility of intra-chip analysis as the reaction proceeds. Infra-red and nuclear magnetic resonance spectroscopies are methods that have been successfully applied to intra-chip reaction monitoring.^{21,22} To date, the use of fluorescence to monitor organic reactions as they proceed in flow remains unexplored.²³

Bioconjugation chemistries are near universally performed as relatively small-scale batch reactions under mild temperature conditions due to the sensitive nature of bio-molecules. Such reactions would appear ideally suited to flow chemistry, though few have been performed in this manner. As example, it has been employed for the rapid synthesis of ¹⁸F radiolabelled proteins used for PET imaging.²⁴ Bovine serine albumin (BSA) and myoglobin proteins have been radiolabelled, within minutes, by amide covalent linkage using the activated ester reagent *N*-succinimidyl 4-[¹⁸F] fluorobenzoate via coupling with lysine residues on the proteins.²⁵ In a similar vein, fluorescent BSA has been produced through in-flow lysine conjugation with fluorescein isothiocyanate.²⁶ A flow apparatus has also been employed to achieve biotin labelling of the antibody trastuzumab Fab. Selective labelling of a specific lysine residue was achievable with a biotin active ester reagent in 30 min with only one biotin unit incorporated per light chain.²⁷ A distinct advantage of such amine coupling reactions is that reactions conditions are mild and do not require catalysis. Biorthogonal reactions can also meet these criteria and they have been explored as alternatives to the traditional conjugation chemistries. For example, ADC and iEDDA reactions can be achieved under the mildest of conditions though substituents strongly influence reaction efficiency.^{28,29} Investigations of biorthogonal reactions using strained alkynes have identified the most suitable reacting partners.³⁰ These reactions can proceed in mild aqueous conditions, without the need for a catalyst, with either azide or tetrazine substrates. To the best of our knowledge, true biorthogonal coupling partners of these types have not been conducted in-flow though a few Cu catalysed variants have been reported.^{26,31,32}

Results and Discussion

Azide functionalized NIR-AZA **2** and the fluorogenic tetrazine NIR-AZA **3** were synthesized following previously published routes.^{12,16} Five BCN derivatives were chosen as strained alkyne substrates, the endo and exo BCN-OH **4a**, **b** were used as model reactants and three

representative bio-substituted derivatives functionalized with carbohydrate **4c** and peptide **4d**, **e** biomolecules (Fig. 4). Derivative **4c** containing a 1,3,4,6-tetra-*O*-acetyl-2-amino-2-deoxy- α -D-glucopyranose unit was selected as the ^{18}F analogue of 2-deoxy-D-glucose is widely used for PET imaging of tumours due to the abnormally high rates of glycolysis of cancer cells.³³ The BCN-peptide **4d** contains the 24-mer linear peptide QIRQQPRDPPTETLELEVSPDPAS-OH (AD-01) which has been shown to be effective for eradicating treatment resistant cancer stem cells.^{34,35} AD-01 was derived by Robson *et al* from the FKBPL protein, and as a therapeutic peptide exhibits antiangiogenic properties and has completed phase 1 clinical trials for the treatment of ovarian cancer. The linking of bio-molecular drugs with imaging agents to combine therapeutic and surgery guiding capacities into a single theranostic entirety is particularly applicable for ovarian cancers.³⁶ The cyclic c(RGDfK) peptide component of **4e** is well recognized for its ability to target integrin transmembrane proteins overexpressed on cancer cells.³⁷ As several c(RGDfK) derivatives have entered clinical trials as tumour therapies and diagnostic imaging agents, covalent labelling with NIR-fluorophores is particularly attractive.³⁸

Synthesis of BCN derivatives **4a-e**

The (bicyclo[6.1.0]non-4-yn-9-yl)methanol endo and exo derivatives **4a**, **b** were synthesized starting from commercially available cyclooctadiene and ethyl diazoacetate as per literature procedures.³⁹ The BCN derivatives **4c-e**, were synthesized using (1R,8S,9s)-bicyclo[6.1.0]non-4-yn-9-ylmethyl *N*-succinimidyl carbonate **5** as the reagent to provide the BCN functionalised biomolecules through a carbamate linkage (Fig. 4). Specifically, synthesis of the BCN substituted biomolecules **4c-e** was achieved as follows; 1,3,4,6-tetra-*O*-acetyl-2-amino-2-deoxy- α -D-glucopyranose was liberated from the hydrochloride salt by sodium hydrogen carbonate and reacted with **5** in the presence of 4-dimethylaminopyridine in DMSO at rt for 2 h. The product was extracted in DCM yielding **4c** a colourless solid in 92%. Therapeutic peptide sequence QIRQQPRDPPTETLELEVSPDPAS-OH was synthesized by solid phase peptide synthesis (SPPS) on an Fmoc-Ser(*t*Bu)-Wang resin.³⁴ The pegylated spacer unit with a terminal protected amine, Fmoc-NH-(PEG)₃-COOH, was coupled to the N-terminus of the resin bound peptide to introduce a distinct spacer and amino conjugation group. Following Fmoc-amine deprotection and cleavage from the resin, the peptide was isolated after extraction and lyophilization. BCN

endo **4a**
exo **4b**

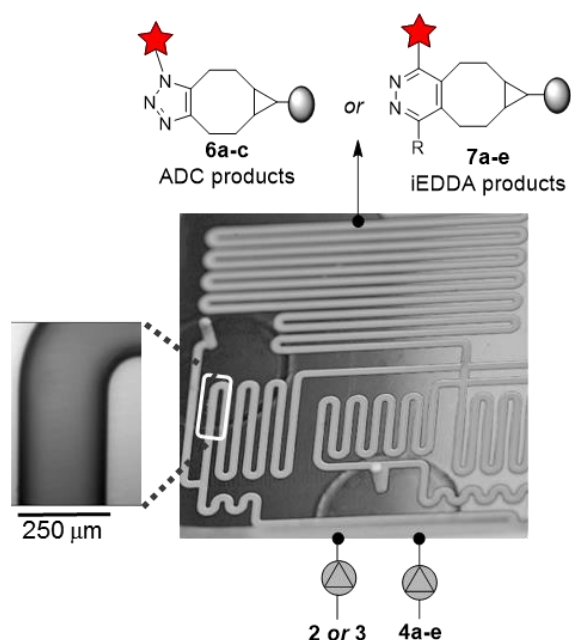
endo **4c**

4d

4e

Similarly, the c(RGDfK) BCN derivative **4e** was readily synthesized by reacting cyclo[Arg-Gly-Asp-D-Phe-Lys(PEG-PEG-NH₂)] with **5** in DMSO for 1 h at rt with product confirmed by HPLC and high resolution MALDI-TOF mass spectrometry (Fig. 4).

In-flow bioconjugations were conducted in either a 1000 or 250 μL glass micro-reactor chip equipped with two piston pumps capable of variable flow rates from 2.5 – 250 $\mu\text{L}/\text{min}$, allowing a range of different residence times to be screened.⁴⁰ Reagent solutions were pumped into the chip via PTFE tubing from pressurized containers. The reactor chip temperature was controlled by a heating/cooling plate and the system was pressurised up to 7 bar by a back pressure regulator. ADC products **6a-c** and iEDAA products **7a-e** were collected and analysed by HPLC (Scheme 1).



Scheme 1. Schematic of the experimental set up for bioconjugations of **2** and **3** in continuous flow. Chip image shows portion of reactor chip used with glass channels of diameter 250 microns.

Initial investigations of flow conditions for the reaction of **2** (0.5 mM) used **4a** as model substrate in a ten-fold equivalence excess at 80 °C. Following a 20 min residence time under these conditions, complete conversion to product was obtained as judged by HPLC analysis (Table 1, entry 1). Decreasing the reaction temperature to 40 °C, with all other conditions maintained, gave a decreased conversion of 60% (entry 2). Further variations were screened with a focus on minimizing the residence time and equivalents required yet maintaining complete conversion (entries 3-5). Optimal conditions were identified as a higher 1 mM concentration of **2** and 5 equiv. of **4a** giving complete conversion to product **6a** in a 10 min residence time (entry 6). Similar trends were seen in the results for the exo isomer **4b** with full conversion maintained at 10 equiv. but lowering to 87% for 5 equiv. with a 10 min residence time while lowering the temperature significantly reduced conversion (entries 8-11). These conditions were then investigated for the glucosamine BCN derivative **4c**. At 5 equiv. 89% conversion to **6c** was achieved which could be increased to 96% by extending the residence time to 15 min (entries 11, 12). Upon reducing the equiv. to 2.5 fold excess the reaction did not reach completion (entries 13, 14). As equimolar

reaction conditions with **2** were proving a challenge and given the high temperature required to achieve complete conversion, reactions with peptide derivatives **4e** and **4f** were not explored. These results show that azide/alkyne conjugation in-flow is achievable, though purification would be required to remove excess reagents and conditions may not be suitable for heat sensitive biomolecules.

Table 1 Flow ADC experiments with azido substituted fluorophore **2**

Entry	2 conc (mM)	4	Equiv. 2 : 4	Product	Temp (°C)	Res. time (min)	Conver. (%) ^a
1	0.5	a	1 : 10	6a	80	20	99
2	0.5	a	1 : 10	6a	40	20	60
3	0.5	a	1 : 10	6a	80	10	>98
4	0.5	a	1 : 5	6a	80	10	64
5	1	a	1 : 2	6a	80	10	80
6	1	a	1 : 5	6a	80	10	96
7	0.5	b	1 : 10	6b	40	20	56
8	1	b	1 : 10	6b	80	10	>98
9	1	b	1 : 5	6b	80	10	87
10	1	b	1 : 10	6b	40	10	54
11	1	c	1 : 5	6c	80	10	89
12	1	c	1 : 5	6c	80	15	96
13	1	c	1 : 2.5	6c	80	10	76
14	1	c	1 : 2.5	6c	80	15	86

^a determined by HPLC detector at 650 nm.

Next, the iEDDA reaction of tetrazine fluorophore **3** with BCN derivatives was investigated at a concentration of 1 mM. Condition screening began with the 40°C reaction of 5 equiv. of **4a** which yielded complete conversion after a 10 min residence time, clearly showing an enhanced reactivity of iEDDA over ADC reactions (Table 2, entry 1). Encouragingly, reduction of residence time to 5 min with a 2-fold excess of **4a** relative to **3** also gave complete conversion (entry 2). Optimal conditions were identified as 1 equiv. of **4a** at 40°C with a 5 min residence time (entry 3), as reduction of the residence time to 2.5 min lowered the conversion to 85% (entry 4). As previously observed, the exo isomer **4b** gave marginally lower 90% conversion under the same conditions (1 equiv., 40°C, 5 min residence time) (entry 5). Pleasingly, the optimal conditions were readily transferred to the glucose and peptide derivatives **4c**, **d** and **e**, each achieving near perfect conversions of 95%, 97% and 97% respectively (entries 6-8). A distinct advantage of the

milder tetrazine iEDDA bioconjugations is that the peptide derivatives **4d** and **e** were viable and these equimolar reactions remove purification requirements.

Table 2 Flow iEDDA experiments with tetrazine substituted fluorophore **3**

Entry	3 conc (mM)	4	Equiv. 3 : 4	Product	Temp (°C)	Res. time (min)	Conver. (%) ^a
1	1	a	1 : 5	7a	40	10	>98
2	1	a	1 : 2	7a	40	5	>98
3	1	a	1 : 1	7a	40	5	95
4	1	a	1 : 1	7a	40	2.5	85
5	1	b	1 : 1	7b	40	5	90
6	1	c	1 : 1	7c	40	5	95
7	1	d	1 : 1	7d	40	5	97
8	1	e	1 : 1	7e	40	5	97

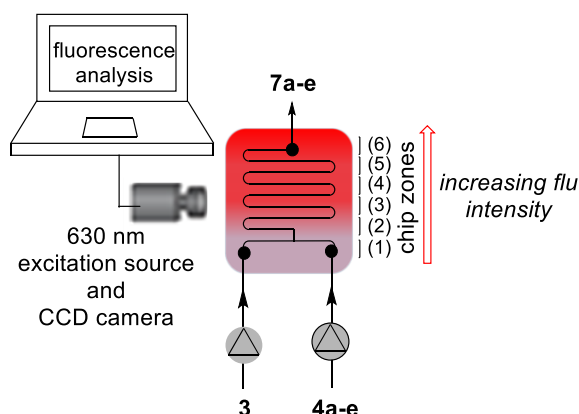
^a determined by HPLC detector at 650 nm.

Intra-chip fluorogenic bioconjugation monitoring

Monitoring the progress of a reaction is fundamental to a successful procedure optimization. Most often for flow reactions, analysis is undertaken ‘post-chip’ by HPLC following exiting of the product from the reaction chip. Other analytical methods such as UV-vis spectroscopy and mass spectrometry can be performed ‘in-line’ by directing the exiting flow path through a specialized cuvette for reaction analysis.^{19a,41} Due to the iEDDA fluorogenic nature of **3**, it was anticipated that an entirely unique ‘intra-chip’ reaction progress monitoring could be achieved for its bioconjugations as fluorescence intensity could be related to conversion to products **7**. Importantly, as there is a continuous and laminar flow of reactants and product through the glass channels of the chip, there is no mixing between different regions of the chip. As such, it was expected that simultaneous monitoring of fluorescence intensity from different chip zones would allow reaction progress to be continually observed from start to completion in real-time. This is of added value for condition sensitive bioconjugations as it may reduce or eliminate the need for purification, minimizes sample handling and allows for continuous monitoring of conversions as the reaction is scaled-out in time.

The apparatus setup for ‘intra-chip’ monitoring consisted of a fibre optic illumination source at 630 nm wavelength and a near infra-red CCD camera positioned above the chip to continuously

collect emissions of wavelength longer than 650 nm from the entire chip as the reaction progressed (Scheme 2). For analysis, the entire chip was software segmented into six field of view (FOV) zones (1-6) of equal area allowing conversion progression to be gauged at different positions (Scheme 2, Fig. 7, inset). Data was analysed with Image-J software to give fluorescence intensity values at the varying zones of the chip. Confirmation that homogeneity of the fluorescence detection at different chip positions was achieved by measuring the different zones when the chip was loaded with solutions of model fluorophore **8** at different concentrations.



Scheme 2. Apparatus setup for intra-chip fluorescence monitoring for continuous flow iEDDA reactions. Fluorescence intensity analysed in Image-J showed a sequential increase for each FOV zone from (1) to (6) due to increased reaction conversion.

Next, a study of concentration versus fluorescence intensity was undertaken using **8** to gain insight into the potential impact of the inner filter effect on intra-chip fluorescence measurement. The inner filter effect is a known occurrence in which fluorescence intensity does not correlate linearly with fluorophore once the concentration exceeds a specific threshold due to reabsorption of emitted light. This, as well as excitation light being attenuated by the sample, particularly affects fluorescence intensity measurements. As optimal flow reaction concentrations are relatively high in the mM range, this potential restriction needed to be considered. Advantageously for flow reactions, the inner filter effect is also dependent upon light path length which in a typical spectrometer cuvette would be 10 mm, whereas the glass

microfluidic reaction channels are only 0.25 mm in diameter (Scheme 1, chip image). For comparison, the emission intensities from **8** at concentrations ranging from 1 μM to 1 mM were recorded in a 1 cm cuvette measured in a spectrometer and the glass reactor chip using the setup described above. The fluorescence intensity versus concentration profile of **8** in a 1 cm path length cuvette shows a reasonably linear profile from 1 to 20 μM , but beyond 30 μM intensity dramatically decreases reaching 15% of maximum at 200 μM (Fig. 5). In contrast, in the reactor chip with channels of 0.25 mm diameter, the concentration range for increasing response was significantly extended up to and beyond 0.2 mM (Fig. 5). As numerous positions within the reaction chip can be read simultaneously, it was anticipated that this would permit reaction progress monitoring even if the fluorescence intensity did not increase in an entirely linear manner with conversion.

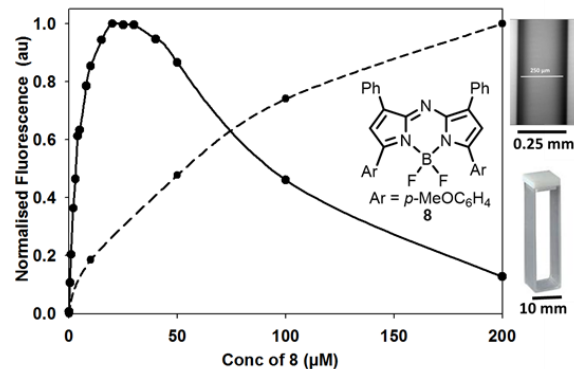


Fig. 5. Fluorescence intensity versus concentration profile of **8** in a 1 mL cuvette (solid line) with excitation at 630 nm and in a reactor chip (dashed line) comprising 0.25 mm diameter glass channels. RHS: top, 0.25 mm micro-reactor chip channel; bottom: 1 cm cuvette.

Reaction conversion tests were carried out to correlate the fluorescence intensity using the representative reactions of **4a** and **4c** with **3** at a concentration of 1 mM. Flow experiments were conducted using **4a** or **c** at 0.25, 0.5, 0.75, and 1 equiv. relative to **3** and the fluorescence readings were recorded in chip FOV zone (6) where the reactions would have reached full conversion. Encouragingly, the intensity values for each experiment, which equate to 25, 50, 75 and 100%

conversions, were distinguishable from each other at the optimal reaction concentration of 1mM (Fig. 6).

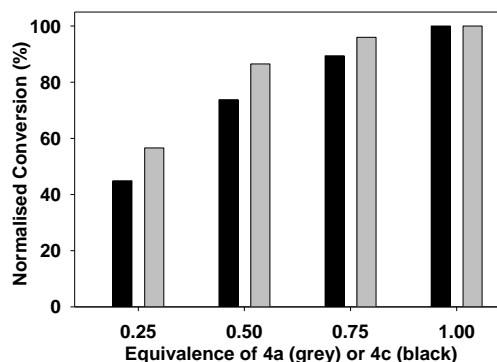


Fig. 6. Fluorescence intensity data analysis of reactor chip FOV zone (6) represented as bar graph for the reaction of **3** with varying equivalence of **4a** (grey) and **4c** (black).

Next, under the optimized reaction conditions (1 mM conc, 1:1 equiv, 40 °C, 5 min) the in-flow reactions of **3** with **4a**, **4c** and **4e** were analysed for their fluorescence intensity simultaneously in chip zones (1) to (6). Plotting of the fluorescence intensities for each zone area showed how intensity increased in each subsequent zone as conversion to products increased until it plateaued at completion (Fig. 7).

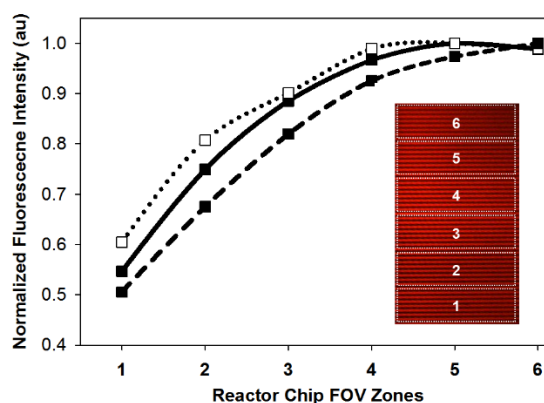


Fig. 7. Fluorescence intensity readouts at chip FOV zones (1) to (6) for 1 mM concentration reaction of **3** with **4a** (dotted line), **4c** (solid line) and **4f** (dashed line). Flow conditions 1:1 equiv. of reagents, 40 °C, 5 min residence time. Inset shows fluorescent image of glass reactor chip with FOV zones used for analysis.

Looking to the future, it could be envisaged that this ability to intra-chip monitor reaction progress could be used to make the system fully automated with continuous monitoring as a reaction is scaled-out in time. A calibrated fluorescence readout could feed back to a reaction control system to alter parameters such as flow rates, residence times and temperatures as required and could lead to fully automated self-monitoring flow synthesis.

Conclusions

In conclusion, an in-flow study of azide and tetrazine cycloadditions with functionalized strained alkyne substrates has shown the suitability of these reactions for bioconjugation of NIR-AZA fluorophores to biomolecules. Optimal reaction conditions for tetrazine / BCN cycloadditions were very favourable, requiring only a 5 min residence time at a mild 40 °C. The combination of in-flow techniques with iEDDA tetrazine chemistry is very applicable to bioconjugation reactions. Due to the fluorogenic nature of the tetrazine-NIR-AZA derivative, it was possible to show for the first time that increasing fluorescence intensity could be exploited for intra-chip reaction monitoring. This advantageous feature is currently being progressed towards self-optimizing reactions in which a fluorescence signature of the product can be distinguished from reacting substrates, the results of which will be reported upon in due course.

Author Contributions

SF contributed experimental methodology, data curation and formal analysis. DFOS conceived the project, contributed to project administration, funding and resources acquisition and supervision. The manuscript was written through contributions of both authors.

Conflicts of Interest

Authors declare that no conflicts of interest exist.

Acknowledgements

The authors acknowledge the Synthesis and Solid State Pharmaceutical Centre (SSPC) and Science foundation Ireland for funding support, grant number 12/RC/2275_P2. Thanks to Dr. Gary

Hessman, Trinity College Dublin and James Flynn, Dr. Edel Durack, University of Limerick for MS analysis. Thanks to Dr. Dan Wu, RCSI, for supply of compound **3**. Thanks to the RCSI Automated Biopolymer and Biomaterials Synthesis facility for peptide synthesis.

Supplementary Information

Electronic supplementary information (ESI) available: All experimental protocols, analytical data and spectra. See DOI:....

References

1. (a) K.M. Dean and A.E. Palmer, *Nat. Chem. Biol.* 2014, **10**, 512-523; (b) J. Kalia and R.T. Raines, *Curr. Org. Chem.* 2010, **14**, 138-147.
2. S. Wäldchen, J. Lehmann, T. Klein, S. van de Linde and M. Sauer, *Sci. Rep.* 2015, **5**, 15348.
3. M. Baker, *Nature* 2010, **466**, 1137-1138.
4. R.R. Zhang, A.B. Schroeder, J.J. Grudzinski, E.L. Rosenthal, J.M. Warram, A.N. Pinchuk, K.W. Eliceiri, J.S. Kuo and J.P. Weichert, *Nat. Rev. Clin. Oncol.* 2017, **14**, 347-364.
5. R.A. Cahill, D.F. O'Shea, M.F. Khan, H.A. Khokhar, J.P. Epperlein, P.G. Mac Aonghusa, R. Nair and S.M. Zhuk, *Brit. J. Sur.*, 2020, **108**, 5-9.
6. (a) L.S.F. Boogerd, C.E.S. Hoogstins, D.P. Schaap, M. Kusters, H.J.M. Handgraaf, M.J.M. van der Valk, D.E. Hilling, F.A. Holman, K.C.M.J. Peeters, J.S.D. Mieog, C.J.H. van de Velde, A. Farina-Sarasqueta, I. van Lijnschoten, B. Framery, A. Pèlegri, M. Gutowski, S.W. Nienhuijs, I.H.J.T. de Hingh, G.A.P. Nieuwenhuijzen, H.J.T. Rutten, F. Cailler, J. Burggraaf and A.L. Vahrmeijer, *Lancet Gastro. Hepat.* 2018, **3**, 181-191. (b) L.E. Amberts, M. Koch, J.S. de Jong, A.L.L. Adams, J. Glatz, M.E.G. Kranendonk, A.G.T. Terwisscha van Scheltinga, L. Jansen, J. de Vries, M.N. Lub-de Hooge, C.P. Schröder, A. Jorritsma-Smit, M.D. Linssen, E. de Boer, B. van der Vegt, W.B. Nagengast, S.G. Elias, S. Oliveira, A.J. Witkamp, W.P.T.M. Mali, E. Van der Wall, P.J. van Diest, E.G.E. de Vries, V. Ntziachristos and G.M. van Dam, *Clin. Cancer Res.* 2017, **23**, 2730. (c) S.E. Miller, W.S. Tummers, N. Teraphongphom, N.S. van den Berg, A. Hasan, R.D. Ertsey, S. Nagpal, L.D. Recht, E.D. Plowey, H. Vogel, G.R. Harsh, G.A. Grant, G.H. Li and E.L. Rosenthal, *J. Neuro-Oncol.*, 2018, **139**, 135-143.

7. M. Gao, F. Yu, C. Lv, J. Choo and L. Chen, *Chem. Soc. Rev.* 2017, **46**, 2237-2271.
8. D. Wu, H.C. Daly, M. Grossi, E. Conroy, B. Li, W.M. Gallagher, R. Elmes and D.F. O'Shea, *Chem. Sci.* 2019, **10**, 6944-6956.
9. H.C. Daly, E. Conroy, M. Todor, D. Wu, W.M. Gallagher and D.F. O'Shea, *Theranostics*, 2020, **10**, 3064-3082.
10. S. Cheung, D. Wu, H.C. Daly, N. Busschaert, M. Morgunova, J.C. Simpson, D. Scholz, P.A. Gale, and D.F. O'Shea, *Chem.* 2018, **4**, 879-895.
11. D. Wu, S. Cheung, M. Devocelle, L.J. Zhang, Z.-L. Chen and D.F. O'Shea, *Chem. Commun.* 2015, **51**, 16667-16670.
12. D. Wu, S. Cheung, R. Daly, H. Burke, E.M. Scanlan and D.F. O'Shea, *Eur. J. Org. Chem.* 2014, **31**, 6841-6845.
13. D. Wu, S. Cheung, C.J. O'Sullivan, Y. Gao, Z.-I. Chen and D.F. O'Shea, *RSC Adv.* 2016, **6**, 87373-87379.
14. M.H.Y. Cheng, A. Maruani, H. Savoie, V. Chudasama and R.W. Boyle, *Org. Biomol. Chem.* 2018, **16**, 1144-1149.
15. J. Pliquett, A. Dubois, C. Racœur, N. Mabrouk, S. Amor, R. Lescure, A. Bettaïeb, B. Collin, C. Bernhard, F. Denat, P.S. Bellaye, C. Paul, E. Bodio and C.A. Goze, *Bioconjugate Chem.* 2019, **30**, 1061-1066.
16. D. Wu, and D.F O'Shea, *Chem. Commun.* 2017, **53**, 10804-10807.
17. E. Kozma and P. Kele, *Org. Biomol. Chem.* 2019, **17**, 215-233.
18. J. Dommerholt, O. van Rooijen, A. Borrmann, C.F. Guerra, F.M. Bickelhaupt and F.L. van Delft, *Nat. Commun.* 2014, **5**, 5378.
19. (a) M. Trojanowicz, *Molecules*, 2020, **25**, 1434; (b) M. Guidi, P.H. Seeberger and Kerry Gilmore, *Chem. Soc. Rev.*, 2020, **49**, 8910—8932.
20. R. Porta, M. Benaglia and A. Puglisi, *Org. Process Res. Dev.* 2015, **20**, 2-25.
21. A.J Oosthoek-de Vries, P.J. Nieuwland, J. Bart, K. Koch, J.W.G. Janssen, P.J.M. van Bentum, F.P.J.T. Rutjes, H.J.G.E. Gardeniers and A.P.M. Kentgens, *J. Am. Chem. Soc.* 2019, **141**, 5369-5380.

22. M. Bomers, B. Charlot, F. Barho, A. Chanuel, A. Mezy, L. Cerutti, F. Gonzalez-Posada and T. Taliercio, *React. Chem. Eng.* 2020, **5**, 124-135.
23. To the best of our knowledge intra-chip fluorescence monitoring has not been applied to continuous flow organic reactions. For examples of in-flow fluorescence sensor and quenching studies see; (a) S.A. Pfeiffer and Stefan Nagl, *Methods Appl. Fluoresc.* 2015, **3**, 034003. (b) L. Gitlin, C. Hoera, R.J. Meier, S. Nagl and D. Belder, L. Gitlin, C. Hoera, R.J. Meier, S. Nagl and D. Belder, *Lab Chip*, 2013, **13**, 4134–4141. (c) K.P.L. Kuijpers, C. Bottecchia, D. Cambié, K. Drummen, N.J. König, and T. Noël, *Angew. Chem. Int. Ed.* 2018, **57**, 11278–11282.
24. M.M. Sebeika, N.G. Gedeon, S. Sadler, N.L. Kern, D.J. Wilkins, D.E. Bell and G.B. Jones, *J. Flow Chem.* 2015, **5**, 151-154.
25. H. Kimura, K. Tomatsu, H. Saiki, K. Arimitsu, M. Ono, H. Kawashima, R. Iwata, H. Nakanishi, E. Ozeki, Y. Kuge and H. Saji, *PloS ONE* 2016, **11**, e0159303.
26. A.R. Bogdan and N.W. Sach, *Adv. Synth. Catal.* 2009, **351**, 849-854.
27. G.H. Pham, W. Ou, B. Bursulaya, M. DiDonato, A. Herath, Y. Jin, X. Hao, J. Loren, G. Spraggon, A. Brock, T. Uno, B.H. Geierstanger and S.E. Cellitti, *ChemBioChem*, 2018, **19**, 799-804.
28. (a) M.F. Debets, S.S. van Berkel, J. Dommerholt, A.J. Dirks, F.P.J.T Rutjes and F.L. van Delft, *Acc. Chem. Res.* 2011, **44**, 805-815. (b) C.S. McKay and M.G. Finn, *Chem. Biol.* 2014, **21**, 1075-1101.
29. V. Terzic, G. Pousse, R. Méallet-Renault, P. Grellier and J. Dubois, *J. Org. Chem.* 2019, **84**, 8542-8551.
30. M.L.W.J Smeenk, J. Agramunt and K.M. Bonger, *Curr. Opin. Chem. Biol.* 2021, **60**, 79-88.
31. M. Teci, M. Tilley, M.A. McGuire and M.G. Organ, *Org. Process Res. Dev.* 2016, **20**, 1967-1973.
32. M.N. Tahir, R.-U. Qamar, A. Adnan, E. Cho and S. Jung, *Tetrahedron Lett.* 2013, **54**, 3268-3273.
33. D. Zhang, J. Li, F. Wang, J. Hu, S. Wang and Y. Sun, *Cancer Lett.* 2014, **355**, 176–183.

34. L. McClements, A. Yakkundi, A. Papaspyropoulos, H. Harrison, M.P. Ablett, P.V. Jithesh, H.D. McKeen, R. Bennett, C. Donley, A. Kissenpfennig, S. McIntosh, H.O. McCarthy, E. O'Neill, R.B. Clarke and T. Robson, *Clin. Cancer Res.* 2013, **19**, 3881-3893.
35. L. McClements, S. Annett, A. Yakkundi, M. O'Rourke, A. Valentine, N. Moustafa, A. Alqudah, B.M. Simões, F. Furlong, A. Short, S.A. McIntosh, H.O. McCarthy, R.B. Clarke and T. Robson, *BMC Cancer*, 2019, **19**, 351.
36. K. Kleinmanns, V. Fosse, B. Davidson, E. G. de Jalón, O. Tenstad, L. Bjørge and E. McCormack, *EBioMedicine*, 2020, **56**, 102783.
37. (a) J.S. Desgrosellier and D.A. Cheresch, *Nat. Rev. Cancer*, 2010, **10**, 9-22. (b) A.J. Beer and M. Schwaiger, *Cancer Metast. Rev.*, 2008, **27**, 631-644.
38. X. Dou, T. Nomoto, H. Takemoto, M. Matsui, K. Tomoda, and N. Nishiyama, *Sci. Rep.* 2018, **8**, 8126.
39. J. Dommerholt, S. Schmidt, R. Temming, L.J.A. Hendriks, F.P.J.T. Rutjes, J.C.M. van Hest, D.J. Lefeber, P. Friedl and F.L. van Delft, *Angew. Chem., Int. Ed.* 2010, **49**, 9422-9425.
40. For more details of the flow system used see; T. Tricotet and D.F. O'Shea, *Chem. Eur. J.* 2010, **16**, 6678 – 6686.
41. B.P. Loren, M. Wleklinski, A. Koswara, K. Yammine, Y. Hu, Z.K. Nagy, D.H. Thompson and R.G. Cooks, *Chem. Sci.*, 2017, **8**, 4363–4370.